

See discussions, stats, and author profiles for this publication at: <https://www.researchgate.net/publication/24392613>

Structure–Activity Relations of Nanolipoblockers with the Atherogenic Domain of Human Macrophage Scavenger Receptor A

ARTICLE *in* BIOMACROMOLECULES · MAY 2009

Impact Factor: 5.75 · DOI: 10.1021/bm8014522 · Source: PubMed

CITATIONS

20

READS

16

4 AUTHORS, INCLUDING:



Sandhya Kortagere

Drexel University College of Medicine

46 PUBLICATIONS 695 CITATIONS

[SEE PROFILE](#)



William Welsh

Rutgers, The State University of New Jersey

139 PUBLICATIONS 3,653 CITATIONS

[SEE PROFILE](#)



Prabhas V Moghe

Rutgers, The State University of New Jersey

106 PUBLICATIONS 1,707 CITATIONS

[SEE PROFILE](#)



NIH Public Access

Author Manuscript

Biomacromolecules. Author manuscript; available in PMC 2010 June 8.

Published in final edited form as:
Biomacromolecules. 2009 June 8; 10(6): 1381–1391. doi:10.1021/bm8014522.

Structure Activity Relations of Nanolipoblockers with the Atherogenic Domain of Human Macrophage Scavenger Receptor

A

Nicole Plourde[†], Sandhya Kortagere^{§,§}, William Welsh[§], and Prabhas Moghe^{†,‡,*}

[†] Department of Chemical and Biochemical Engineering, Rutgers University, Piscataway, NJ 08854

[‡] Department of Biomedical Engineering, Rutgers University, Piscataway, NJ 08854

[§] Department of Microbiology and Immunology, Drexel University College of Medicine, Philadelphia, PA 19129

[§] Department of Pharmacology, Environmental Bioinformatics & Computational Toxicology Research Center University of Medicine and Dentistry of New Jersey (UMDNJ), Robert Wood Johnson Medical School, Piscataway, NJ 08854

Abstract

Oxidized low density lipoprotein (oxLDL) uptake by macrophages is mediated by scavenger receptors and leads to unregulated cholesterol accumulation. Micellar nanolipoblockers (NLBs) consist of alkyl chains and polyethylene glycol on mucic acid. NLBs functionalized with anionic groups inhibit oxLDL uptake via the scavenger receptor A (SR-A). Molecular modeling and docking approaches were used to understand the structure-activity relationship (SAR) between NLBs and SR-A. Six NLB models were docked to the SR-A homology model to investigate charge placement and clustering. NLB models with the most favorable binding energy were also the most effective oxLDL inhibitors in THP-1 macrophages. Mutant SR-A models were generated by replacing charged residues with alanine. All charged residues in the region were necessary, with Lys60, Lys63 and Lys66 having the greatest effect on binding. We hypothesize that structural studies aided by theoretical modeling and docking can be used to design promising NLB candidates with optimal binding properties.

Keywords

Atherosclerosis; low density lipoproteins; nanolipoblocker; scavenger receptor model; docking and scoring

Introduction

Atherosclerosis is triggered by complex interactions between macrophages, smooth muscle cells and extracellular matrix molecules, following the pathologic build-up of low density lipoproteins (LDL) within the vascular wall region.¹ This condition leads to coronary heart disease, which is currently the leading cause of death in America (American Heart Association 2007). The progression towards disease begins with LDL, the major carriers of cholesterol in the blood plasma, which enter the arterial wall from the blood stream where it is sequestered by extracellular matrix molecules and becomes modified (oxidized).^{2, 3} Upon modification,

*AUTHOR EMAIL ADDRESS: E-mail: moghe@rci.rutgers.edu.

the oxidized LDL (oxLDL) is free to interact with intimal macrophages.⁴ OxLDL uptake is mediated by scavenger receptors, which unlike the receptors for native LDL, are not down-regulated.⁵ This leads to unregulated cholesterol accumulation and results in the formation of foam cells and fatty streaks, which are the earliest visible atherosclerotic lesions.^{5, 6} The two principal receptors involved in oxLDL uptake are SR-A and a class B scavenger receptor-CD36, and account for the majority of modified LDL uptake (75–90%) and degradation, as demonstrated by knockout mice lacking both SR-A and CD36 receptors.⁷ A characteristic of SR-A is the mediation of uptake and degradation of modified proteins and several polyanionic ligands in the absence of structural similarities.^{8–10} Ligand binding is thought to be mediated through electrostatic interactions between the arginine and lysine residues in the collagenous domain and negative charges on the ligands.¹¹ Interactions of ligands with CD36 are generally hydrophobic and only somewhat mediated by charge.¹² A cluster of amino acids has been proposed to be membrane-associated and form hydrophobic pockets on the CD36 receptor.¹³

One promising avenue of interest in the treatment and prevention of cardiovascular disease is the use of a scavenger receptor inhibitor to prevent oxLDL uptake via scavenger receptors. OxLDL (and not native LDL) stimulates foam cell formation through binding to macrophage scavenger receptors, which leads to unregulated cholesterol accumulation.^{5, 6} Therefore, any approach directed at lowering LDL accumulation within the vascular intima should prevent this uncontrolled uptake. Previously, synthetic compounds that can bind to scavenger receptors, potentially blocking oxidized LDL entry into cells have been investigated.^{14–17} Synthetic oxidized phospholipids (oxidized phosphocholine) cross-linked to a hexapeptide or bovine serum albumin (BSA) have been used as pattern recognition ligands for CD36 and have been shown to viably inhibit the binding of oxLDL to CD36 expressing cells.¹⁴ In addition, sulfatide derivatives for the targeting of SR-A have been synthesized and investigated and have been shown to reduce acetylated LDL binding and uptake in a concentration-dependent manner.¹⁵

A unique class of multifunctional polymers, amphiphilic scorpion-like macromolecules (AScM) have been described previously and will be referred to as nanolipoblockers (NLBs).¹⁸ The NLBs are micellar aggregates of unimers identified as M12P5 which corresponds to a mucic acid (M) with aliphatic acid chains of 12 carbons (12) and polyethylene glycol (PEG) chains (P) with a molecular weight of 5 kDa (5) (Figure 1). These building blocks are naturally occurring or biocompatible compounds and are connected via biodegradable ester bonds. PEG contributes to the polymer's hydrophilicity and is used to prevent the non-specific adsorption of proteins. Mucic acid is a multi-hydroxylated saccharide providing reaction sites for further polymer modification, and aliphatic acid chains control the polymer hydrophobicity. The branched hydrophobic core aids in particle stability, as seen by the low critical micelle concentration (CMC) ($1.25 * 10^{-7}$ M), as well as increases the micelle's capacity to self-assemble.¹⁸ Cytotoxicity studies have shown that the micelles are not cytotoxic up to concentrations well above those used *in vitro* (10^{-4} M).¹⁹ The micelle also has a small aggregation diameter (~20 nm). Current studies have focused on using NLBs as scavenger receptor-blockers. In studies with mouse IC21 peritoneal macrophages the NLBs have been functionalized with a carboxylic acid which reduced oxLDL uptake by up to 80%, via the SR-A and CD36 scavenger receptors.^{20, 21} It is hypothesized that the collagenous region of mouse macrophage SR-A is responsible for NLB binding as it has been shown to be the region responsible for oxLDL binding and contains a cluster of positively charged amino acids which bind to anionic ligands.^{22–25}

Although previous studies provide information on the correlation between particle design and the prevention of oxLDL uptake^{20, 21, 26, 27}, the mechanistic contribution of sub-domains of the macromolecules are not well understood thus making the current trial and error pipeline from NLB design to *in vitro* testing time consuming and inefficient. Therefore, the present SAR studies are targeted at understanding the nature of interactions between the collagen

domain of the scavenger receptor SR-A and the modeled NLBs, as illustrated in Figure 1. The results from this study will further enable the screening of numerous virtually designed NLBs and obviate the need to synthesize structures with suboptimal binding properties. Analysis will involve both *in vitro* studies as well as atomistic molecular modeling simulations of macrophages and NLB interactions. While atomistic models are insightful, they can be somewhat limited in their ability to fully capture the entire nanoparticle dynamics. However, the insights gained from the SAR of modeled micelle systems with SR-A will be useful to design future *in-silico* analysis of the complete NLB.

Methods

Nanolipoblocker synthesis

Structures were prepared as previously described.^{18, 21, 27} The major reactants included 5000 Da heterobifunctional poly(ethylene glycol) (NH₂-PEG-COOH) (Nektar, San Carlos, CA), 4-(dimethylamino)pyridinium p-toluenesulfonate (DPTS) and carboxylate-terminated poly(ethylene glycol) (PEG-COOH 5000 MW) (Sigma, St. Louis, MO). All PEG reagents were dried by azeotropic distillation with toluene. All other reagents and solvents were purchased from Aldrich and used as received.

Nanolipoblocker Characterization

Chemical structures and compositions were confirmed by ¹H and ¹³C NMR spectroscopy with samples (~ 5–10 mg/ml) dissolved in CDCl₃-d solvent on Varian 400 MHz spectrometers, using tetramethylsilane as the reference signal. IR spectra were recorded on a Mattson Series spectrophotometer (Madison Instruments, Madison, WI) by solvent (methylene chloride) casting on a KBr pellet. Negative ion-mass spectra were recorded with a ThermoQuest Finnigan LCQTM DUO System (San Jose, CA) that includes a syringe pump, an optional divert/inject valve, an atmospheric pressure ionization (API) source, a mass spectrometer (MS) detector, and the Xcalibur data system. Meltemp (Cambridge, Mass) was used to determine the melting temperatures (T_m) of all the intermediates.

Gel permeation chromatography (GPC) was used to obtain molecular weight and polydispersity index (PDI). It was performed on Perkin-Elmer Series 200 LC system equipped with PI gel column (5 µm, mixed bed, ID 7.8 mm, and length 300 mm) and with a Water 410 refractive index detector, Series 200 LC pump and ISS 200 Autosampler. Tetrahydrofuran (THF) was the eluent for analysis and solvent for sample preparation. Sample was dissolved into THF (~ 5 mg/ml) and filtered through a 0.45 µm PTFE syringe filter (Whatman, Clifton, NJ) before injection into the column at a flow rate of 1.0 ml/min. The average molecular weight of the sample was calibrated against narrow molecular weight polystyrene standards (Polysciences, Warrington, PA).

Experimental Cell Studies

All studies of NLB interactions with living cells were conducted using human THP-1 monocytes (ATCC, Manassas, VA). The cells were propagated in culture using RPMI-1640 media (ATCC, Manassas, VA) containing 10% fetal bovine serum and 1% penicillin/streptomycin at 37°C in 5% CO₂. Differentiation of THP-1 monocytes into macrophages was induced by plating the cells at a density of 9.0 × 10⁴ cells/cm² in the presence of 16 nM phorbol myristate acetate (PMA) for 14 hr and an additional 58 hr with media before experimental use. As described previously²⁶, oxLDL was generated by incubating 50 µg/ml LDL purified from human plasma (Molecular Probes Eugene, OR) with 10 µM CuSO₄ at 37 °C for 18 hr exposed to air.^{28, 29} Oxidation was terminated with 0.01% w/v EDTA (Sigma, St. Louis, MO).

In the uptake studies a 10^{-4} M stock solution of NLBs was freshly prepared in RPMI-1640 medium no more than 7 days before experimental use. The NLBs were diluted with additional RPMI-1640 or oxLDL to create a final NLB concentration of 10^{-6} M. 10 µg/ml oxidized fluorescently labeled BODIPY-LDL combined with NLBs was incubated with THP-1 cells at 37 °C in presence of serum free medium. Following incubation with oxLDL and NLBs, the cells were washed twice with serum free RPMI containing 0.4% bovine serum albumin (BSA) (Sigma, St. Louis, MO) and twice with serum free RPMI, to remove unbound labeled oxLDL. The cells were gently fixed in a 3.7% formaldehyde solution for 20 min at room temperature and the cell associated fluorescence was quantified by imaging the cells using a Nikon Eclipse TE2000-S fluorescent microscope and Image Pro Plus 5.1 software (Media Cybernetics, San Diego, CA). The levels of oxLDL uptake were normalized to those obtained in the absence of NLBs. Each condition was performed in triplicate and five fields were captured per well.

The role of scavenger receptors in NLB uptake by THP-1 human macrophages was ascertained by incubating the cells with 10 µg/mL primary antibodies to SR-A (Monoclonal Mouse Anti-human0 SR-A/MSR1 Antibody, R&D Systems, Minneapolis, MN) and CD36 (Monoclonal Rat Anti-human CD36/SR-B3 Antibody, R&D Systems, Minneapolis, MN) for 45 min at 37 °C to block receptor availability. To avoid any nonspecific reaction between the IgG isotypes and the macrophage cells, isotype controls were included where the SR-A and CD36 antibodies were replaced with purified mouse IgG₁ and purified rat IgG_{2b} respectively (Invitrogen, Carlsbad, CA). The anionic NLBs were fluorescently labeled with cationic Texas Red hydrazide dye (Molecular Probes, Eugene, OR), using carbodiimide chemistry as previously published.²¹ For cellular uptake studies a 5% solution of fluorescently labeled NLBs was mixed with unlabeled particles dissolved in serum-free RPMI. The cells were incubated with 10^{-6} M fluorescently labeled NLBs in serum-free RPMI for 2 hr at 37 °C in the presence of additional antibodies or controls to guarantee continuous receptor blocking. Following incubation, the cells were washed twice with serum free RPMI containing 0.4% BSA (Sigma, St. Louis, MO) and twice with serum free RPMI alone. The cells were gently fixed in a 3.7% formaldehyde solution for 20 min at room temperature and the cell associated fluorescence was quantified by imaging the cells using a Nikon Eclipse TE2000-S fluorescent microscope and Image Pro Plus 5.1 software (Media Cybernetics, San Diego, CA). Each condition was performed in triplicate and five fields were captured per well.

Statistical Analysis

Each *in vitro* experiment was performed at least twice and three replicate samples were investigated in each experiment. The results were then analyzed using analysis of variance (ANOVA). Significance criteria assumed a 95% confidence level ($P<0.05$). Standard error of the mean is reported in the form of error bars on the graphs of the final data.

Molecular Modeling

The NLBs were built according to their chemical structures illustrated in Figure 2 using the build module in molecular operating environment (MOE) (Chemical Computing Group, Inc., Montreal, Canada). The model NLB molecules were parameterized for Amber99³⁰ force field and energy minimized until convergence (grad = 0.001) was attained.

The primary sequence of the human SR-A receptor was retrieved from the National Center for Biotechnology Information (NCBI) Entrez protein database (P21757 – Macrophage scavenger receptor types I and II) and the sequence was matched with similar sequences of proteins from the Protein Data Bank (PDB) using NCBI Basic Local Alignment Search Tool (BLAST).³¹ Pairwise sequence alignment of the template sequences with the SR-A collagen-like domain sequence was completed using CLUSTALW.³² For further analysis, the secondary structures of both SR-A and collagen type I, chain A³³ (1Y0FA) were determined through PSIPRED,

which maps sequences into regions of helices, coils, or strands.^{34, 35} The structures were mapped similarly and throughout the collagen-like domain and the corresponding region of collagen type I chain A the regions contained coils with high prediction confidence. The PDB file for collagen type I chain A contained only the protein backbone therefore the side chains were modeled using SYBYL (Ver 8.0 Tripos Inc., St. Louis, Missouri, USA) and energy minimized using steepest descent method until convergence was attained. The 3D homology model of the SR-A collagen-like domain was generated using the program MODELLER³⁶ with collagen type I chain A as template. MODELLER program utilizes spatial constraints derived from template structures for the generation of 3D model structures of proteins.³⁶ The resulting 3D model is obtained by 1) calculating distance and dihedral angle restraints from the aligned target and template 3D structure, 2) utilizing an objective function of combined spatial restraints and CHARMM energy terms to impose proper stereochemistry³⁷, and 3) optimizing the objective function in Cartesian space through applying the variable target function method³⁸ utilizing techniques of conjugate gradients and molecular dynamics with simulated annealing.³⁶ The resulting PDB file of the collagen-like region of SR-A was parameterized for Amber99³⁰ force field and energy minimized until convergence (grad = 0.001) was attained and further refined using molecular dynamics simulation using AMBER³⁹ program at 300K with a production run of 500 ps. Further, mutants were generated by substituting segments of the known binding region in the human collagen-like domain important for oxLDL binding (three lysines and two arginines^{22–25, 40}) with alanines using SYBYL8.0 and refined applying the same process described previously for the wild-type.

Docking and Scoring

The models of NLBs were docked to collagen-like domain of SR-A using GOLD v3.2.⁴¹ The GOLD program employs a genetic algorithm for docking flexible ligands into partially flexible receptor sites. The binding cavity was defined as residues Arg45 – Ser68 with an active site radius of 15 Å° such that all residues important for oxLDL binding were included. Dockings were performed with standard default settings; population size of 100, selection pressure of 1.1, number of operations was 100,000, number of islands was 5, and a niche size of 2. Twenty independent docking runs were performed for each NLB. In the absence of any general rule to choose the number of conformations in GOLD, we have used 20 runs that optimized the computational time required to dock and score non-redundant conformations. The docked pairs were ranked based on each GoldScore, which is a scoring function based on H-bonding energy, van der Waals energy and ligand torsion strain. In most cases the best ranking conformation of the NLB illustrated the most preferred conformation to interact with scavenger receptor. The binding energy was computed for the refined complexes using Equation 1.

$$\Delta E_{binding} = \Delta E_{complex} - \Delta E_{SR-A} - \Delta E_{NLB}$$
Equation 1

Where $\Delta E_{complex}$ is the energy of the NLBs docked to collagen-like domain of SR-A, ΔE_{SR-A} is the energy of the homology model of the scavenger receptor collagen-like domain, and ΔE_{NLB} is the energy of the NLB. Each structure (NLB model, homology model of the SR-A collagen-like domain, and the docked conformation of the pair) was parameterized using Amber99³⁰ force field and energy minimized until convergence (grad = 0.001) was attained. These minimized energies were used to estimate the binding energy from Equation 1.

Results and Discussion

Identification of Scavenger Receptors Involved in Cell-NLB Interactions

To identify which receptor(s) were involved in the interaction between macrophage cells and NLBs, the role of scavenger receptors were investigated through the use of selective blocking with antibodies. Similar to knockout studies, the importance of each receptor can be inferred from the binding observed with receptor blocking compared to binding detected without receptor blocking. Previously published results on mouse IC21 macrophages showed that both CD36 and SR-A were actively involved in mediating the uptake of anionic NLBs.²¹ The NLBs tested had one carboxylate on the mucic acid (1cM) as the anionic NLB and zero carboxylates on the mucic acid (0cM) as the neutral control (Figure 2). The role of scavenger receptors in NLB uptake by THP-1 human macrophages was ascertained by incubating the cells with primary antibodies to SR-A and CD36 and their isotype controls in addition to NLBs for 1 hr (Figure 3). The basal binding of 0cM was minimal and no variation was observed in the scavenger receptor blocking conditions. This suggested that the interaction between 0cM and THP-1 macrophages was negligible, reinforcing the finding that 0cM was not effective at reducing oxLDL internalization.^{20, 21} Further, no change was seen between the blocking and non-blocking conditions, implying that the trivial binding noted was not SR-A specific. In addition, when both SR-A and CD36 receptors were antibody-blocked, binding of both 1cM and 0cM was minimal and no significant difference was detected between the two conditions. This implied that the modest binding that was identified was independent of the anionic charge on NLBs. The finding that some binding could still be noted when both SR-A and CD36 were blocked may suggest the involvement of other scavenger or cell-surface receptors.

Blockage of either scavenger receptor led to a decrease in binding of 1cM that implied a mechanism for NLB uptake and oxLDL inhibition. However, most importantly the 1cM binding observed when both SR-A and CD36 were blocked was no less than the 1cM binding detected with the blocking of only SR-A. Therefore, no additional 1cM binding obstruction was gained with the addition of the CD36 antibody. This indicated that for THP-1 macrophage cells the primary scavenger receptor responsible for anionic NLB binding was SR-A, and thus should be the focus of further investigation.

SAR of NLBs with Macrophage Scavenger Receptors

The role of the positioning and clustering of the anionic (carboxylate) group of the NLBs on the inhibition of oxLDL uptake in THP-1 macrophages was examined via incubation of the cells with 10^{-6} M NLBs and fluorescent oxLDL for 5 hr at 37 °C (Figure 4). The first generation of NLBs to be investigated included 1cM and 0cM as well as 1 carboxylate on the PEG chain (1cP), and 1 carboxylate on PEG without aliphatic chains (PEG-COOH), as seen in Figure 2. The 1cM and 1cP were used to observe the effect of charge location on NLB binding and uptake and the 0cM served as the neutral control particle. PEG-COOH was used as a non-micellar control as it contained the same functional group and PEG chain length, but did not form micelles in solution.

Results of oxLDL accumulation followed a similar trend as that observed with mouse macrophages and NLBs.²¹ The PEG-COOH macromolecules, which did not self-assemble into micelles, produced minimal inhibition of oxLDL uptake by macrophages. This suggests the importance of organization and clustering of anionic charges for receptor blocking or the requirement of hydrophobic moieties in close proximity to the anionic group. Uncharged NLBs (0cM) had a limited effect in inhibiting oxLDL accumulation, which was dramatically enhanced in the presence of either anionic particle (1cM and 1cP). The NLB containing hydrophobic-bound carboxylate groups (1cM) was the most efficient inhibitor and resulted in a 67% reduction in oxLDL accumulation by macrophage cells. In contrast, the 1cP, which had

the anionic groups conjugated to the hydrophilic domain caused only 41% induced reduction in oxLDL uptake. Given that 1cM and 1cP have similar charge densities as demonstrated previously through zeta potential measurements²⁷, this finding implied that the interaction between the receptor and NLB was not solely charge-based. The enhanced binding may be due to hydrophobic and charge interactions acting in concert for improved inhibitory ability, but could not be confirmed by uptake studies. Hence, molecular modeling and docking simulations were performed to further understand the SAR of the NLBs with SR-A.

Molecular Modeling of NLBs and Scavenger Receptor

The model NLBs, described above, were scaled to contain PEG chain repeats of 20 in place of 115 and aliphatic chains of 2 repeats in place of 4. Two forms of first generation models were chosen to understand the structural interactions of NLBs with SR-A. The first model consisted of a single unimer of the NLB aggregate with varying charge locations corresponding to 0cM, 1cM, 1cP and PEG-COOH, as seen in Figure 2. NLB unimers form micelle aggregates in solution, however it is unknown whether the NLB binds to the SR-A collagenous domain as an aggregate or as single unimers. It is expected that each unimer is active and is able to bind to SR-A. The second model contained two 1cM unimers covalently linked at the aliphatic chain on position 5 and represented a segment of a 1cM NLB aggregate to approximate the behavior of a multi-unimer NLB. While a more robust model would be necessary to fully capture micelle aggregation dynamics, the linked NLB model is a straightforward representation of the behavior of unimers in close proximity.

The three dimensional (3D) structure of SR-A is unknown, however previous work by Doi et al²³ employed a charged collagen model based on poly(L-prolyl-glycyl-L-proline) to investigate the recognition of negatively charged particles by SR-A.⁴² For our studies, a multi-step process was used to match the SR-A sequence with a similar sequence of known structure in order to predict scavenger receptor structure. Residues 812–877 of the collagen-like region of SR-A was modeled, as anionic ligand binding is mediated through the collagenous domain.¹¹ The amino acid sequence for SR-A was matched with similar sequences of proteins using a BLAST³¹ search of the PDB. Two matches with the highest score were the structure of collagen type I, chain A³³ (1Y0FA) and the high resolution crystal structure of an active recombinant fragment of human lung surfactant protein D⁴³ (1PW9), with bit scores of 32.0 and 25.4 respectively. The scores are based on the alignment of similar or identical residues and gaps introduced to align the sequences; higher scores indicate better alignment.³¹

Site-directed mutagenesis studies have shown three lysines and two arginines in the human collagen-like domain to be important for oxLDL binding capability.^{22–25, 40} Based on this evidence, we have hypothesized that the collagen-like domain to be necessary for NLB binding, as NLBs are able to reduce oxLDL accumulation via their interaction with SR-A.²¹ In the region of interest, the alignment between collagen type I chain A and the SR-A collagen-like domain contained two identical matches and two “similar” matches. In addition, the structure of collagen was functionally similar to the collagenous domain of SR-A more so than the fragment of human lung surfactant protein D and therefore collagen type I chain A was chosen as the template for future studies (Figure 5). For further analysis, the secondary structures of both SR-A and collagen type I chain A were determined using PSIPRED³³, which mapped sequences into regions of helices, coils, or strands.^{34, 35} The collagen-like domain of SR-A and the corresponding region of collagen type I chain A contained coils with high prediction confidence. The 3D model of the SR-A collagen-like domain was generated using the program MODELLER³⁶ and refined using energy minimization and molecular dynamics simulations using AMBER³⁹ program (see “Methods”). Further, mutant models of this protein were generated by substituting segments of the known binding region in the human collagen-like domain with alanine that will be further described in detail in the following sections.

Docking and Scoring

It is hypothesized that the 3D structure and chemical composition of the NLBs determine the strength of binding of the NLB to SR-A. The modeled NLBs were docked to SR-A collagen-like domain homology model using GOLD v3.2.⁴¹ The docked pairs were ranked based on each GoldScore. Doi et al²³ speculated that 4 lysines at positions 327, 334, 337, and 340 in bovine scavenger receptor (3 lysines and 1 arginine in human SR-A) were critical for anionic ligand binding and uptake, while Freeman et al²² investigated this further and reported that in addition to these residues, Arg317 was also necessary for modified LDL binding and its deletion led to a decrease in binding. These five residues correspond to Arg45, Arg53, Lys60, Lys63 and Lys66 in our SR-A collagenous domain homology model. For the docking studies the binding pocket was therefore defined by including these five essential residues. Figure 6 illustrates the consensus binding of 20 independent docking runs. There was no consensus orientation or specificity seen with the 20 docking runs of the 0cM NLB model. However, the hydrophobic aliphatic chains occasionally remained close to the positive pocket. This lack of directed specificity with sporadic positioning near the charged residues in the collagenous domain may explain the finding that 0cM exhibits limited blocking of oxLDL accumulation, which was far less than anionic NLBs. It was noted that only 1cM and PEG-COOH appeared to be oriented in a way so as to facilitate binding in the essential region, specifically Lys60. However, only the 1cM, and not the PEG-COOH, prevented the accumulation of oxLDL in the *in vitro* studies. The aliphatic chains seemed to stabilize the long molecule and acted as an anchor between the carboxylate group on the 1cM NLB model and the SR-A collagenous domain homology model. This may be due to interactions between the aliphatic chains and several glycine residues in the SR-A collagenous domain (Figure 5). The bulk of these chains are far removed from the anionic moiety which appeared to instead hinder the binding of 1cP while their removal (as illustrated with PEG-COOH) restored binding. PEG did not appear to be predominantly involved in binding; however it was necessary *in vitro* for micelle formation and protected the anionic moiety from non-specific adsorption of proteins.⁴⁴ The docking of the second model of two 1cM unimers covalently linked at the aliphatic chain on position 5 can be seen in Figure 7. The goal of this model was to represent a section of a 1cM NLB aggregate to approximate the behavior of a multi-unimer NLB. It is noteworthy that when docked, the 2 unimers oriented such that the PEG chains were positioned away from the SR-A collagenous domain and the aliphatic chains formed a “core-like” structure around the binding pocket, specifically Arg53 and Lys60. Thus we hypothesize that the multi-unimer NLB particle binds to the SR-A in a mode where the carboxylates in the micelle core act in concert to interact with the charged region (Arg45 to Glu65) of the collagenous domain of SR-A. Further studies are underway to investigate the viability of using a coarse grain model of the NLB particle and the collagenous domain of SR-A.

The binding energy was computed for each refined complex using Equation 1 and the results are tabulated in Table 1. The energy values reinforce docked observations, in that the NLB models with the most favorable energies were also positioned in a way so as to facilitate binding. Only 1cM and PEG-COOH appeared to be oriented in a way to facilitate binding in the region of 5 positive residues and these were the only NLB models with favorable energies. The binding energies also trend well with the experimental oxLDL uptake data (Figure 4). While the accumulation of oxLDL is not a direct measurement of ligand binding it can be inferred that the NLBs with the most favorable binding energy bind at a higher rate than NLBs with less favorable binding energies and therefore would block more oxLDL from accumulating within the THP-1 macrophages. The 1cM NLB model had both the most favorable binding energy and also prevented the most oxLDL from accumulating *in vitro*. It should be noted that while the energy of the second model of two 1cM unimers covalently linked at the aliphatic chain was very unfavorable, the two unimers would not be covalently linked in actuality but would instead be a fraction of a dynamic micelle. The covalent bond

limited the degrees of freedom, however the NLB mode of binding as a micellar aggregate cannot be ruled out. This was reinforced by the finding that while the PEG-COOH NLB had similar binding energy to the 1cM, it was far less successful at reducing the accumulation of oxLDL *in vitro*. The PEG-COOH lacked only the aliphatic side chains of the 1cM and did not form micelles in solution.²¹ These evidences indicated the necessity of aliphatic arms in an NLB for efficient binding and possibly to the need for a multi-unimer NLB aggregate.

Examination of Multiply-Charged NLBs

In light of the close correlation between the *in vitro* oxLDL accumulation data in THP-1 macrophages and the *in silico* binding energy results, a second generation of NLB configurations were investigated based on the design of the first generation of NLBs. Two multiply-charged (MC) NLBs each containing 2 carboxylate groups were designed to investigate the role of charge clustering and charge location and to assess the ability of the model to predict NLB effectiveness *in vitro*, as seen in Figure 2. Based on the finding that one carboxylate on the mucic acid provided both strong model binding and was an efficient inhibitor of oxLDL *in vitro* (1cM), a MC-NLB containing two carboxylates on the mucic acid (2cM) was modeled. Further, a second MC-NLB containing one carboxylate on the mucic acid and one carboxylate on the PEG chain (1cM1cP) was modeled to investigate the effect of multiple charge placement. As described above, the MC-NLBs were scaled to contain PEG chain repeats of 20 in place of 115 and aliphatic chains of 2 repeats in place of 4. The modeled MC-NLBs were docked to SR-A collagen-like domain homology model using GOLD v3.2⁴¹ and the docked pairs were ranked based on each GoldScore. Figure 8 illustrates the consensus binding of 20 independent docking runs. It can be noted that the flexibility of the PEG chain in the 1cM1cP allowed for at least two predominant binding modes as shown in configurations A and B. In the first mode (Figure 8A), which occurred in 70% of the docking runs, the MC-NLB had a more linear conformation, in which the carboxylates interacted with Arg45 and Gly55. In the second mode (Figure 8B), which was observed in 30% of docking runs, the MC-NLB was seen to fold inwards such that the two carboxylates were proximal and interacted with neighboring residues Pro48, Tyr50, Ala51, Arg53 and Pro54. In contrast, in the 2cM MC-NLB the positioning of the two carboxylate groups on the mucic acid resulted in binding between no more than 1 residue and 1 anionic group, as seen in Figure 8C with Arg53.

The binding energy was computed for each refined complex using Equation 1 and the results are tabulated in Table 1. Of all of the NLB models examined the 1cM1cP MC-NLB model had the most favorable binding energy. In comparison with the 1cM model, the 1cM1cP model had additional interactions with both adjacent and remote residues. These additional large favorable interactions could account for the increase in the binding energy in comparison with 1cM model. The binding of the 2cM NLB model to the collagen-like domain was unfavorable and similar to the value of 0cM binding. This seems inconsistent with the previous finding that carboxylates located on the mucic acid result in favorable binding (1cM) and that increased charge results in increased binding (1cM1cP). There are several explanations for this phenomenon. First, in the 2cM model the carboxylate groups are positioned closely together. This limited the degrees of freedom of the two carboxylates to move and bind more than one residue, compared to the 1cM1cP. Second, internal hydrogen bonding was observed between the carboxylates and the nitrogen at position 4 or the oxygen at position 5 which resulted carboxylates unavailable for binding to SR-A. Third, compared to the other NLB models, the 2cM was less hydrophobic due to the additional anionic charge near the hydrophobic moiety.

The binding energies trend well with the experimental oxLDL uptake data and were validated by the *in vitro* results in Figure 9. Here, the MC-NLBs were compared to the previous gold standard, 1cM, and basal uptake in the presence of no particles. The role of the positioning and clustering of the anionic groups of the MC-NLBs on the inhibition of oxLDL uptake in THP-1

macrophages was examined via incubation of the cells with 10^{-6} M NLBs and fluorescent oxLDL for 5 hr at 37 °C. The 2cM NLB inhibited minimal uptake of oxLDL. This was not surprising as the model binding was found to be similar to that of 0cM. However, *in vitro* 1cM1cP was as effective as, but no more successful than 1cM. The additional carboxylate on the PEG enhanced binding but did not translate to a more effective oxLDL inhibitor. The favorable energetics of 1cM1cP model could be an anomaly of the NLB model design and could vary based on the number of unimers in the model. Overall, the correlation between the MC-NLB modeling results and the *in vitro* results is encouraging and implies that the model is capable of capturing NLB-SR-A collagen-like domain interactions.

Docking and Scoring of Mutants

In an effort to understand the role of the 5 conserved residues on NLB binding, mutants were generated by substituting segments of the known binding region (three lysines and two arginines^{22–25}) with alanines. Initially, 3 mutant models were generated; mutant 1 (replacement of Arg45, Arg53, Lys60, Lys63 and Lys66 with alanine), mutant 2 (replacement of Arg45 and Arg53 with alanine) and mutant 3 (replacement of Lys60, Lys63 and Lys66 with alanine). The 1cM model was chosen as the test NLB because the 1cM had strong interactions with the SR-A collagen-like domain homology model and also had close correlation to the *in vitro* oxLDL uptake results. 1cM was docked to the mutants using GOLD v3.2⁴¹ and the docked pairs were ranked based on GoldScore. Figure 10 illustrates the consensus binding of 20 independent docking runs between the mutants and 1cM. In mutant 1 model all the five charged residues were removed and yet binding was still observed consistently between the carboxylate group and residues Gln62 and Glu65. This finding led to the generation of two additional mutants: mutant 4 (replacement of Gln62 and Glu65 with alanines) and mutant 5 (replacement of Arg45, Arg53, Lys60, Lys63, Lys66, Gln62 and Glu65 with alanines). In mutants 2, 3, and 4, after the removal of charged residues of interest, binding was retained through interactions with the remaining positive amino acids (Lys60, Lys63 and Lys66 in mutant 2, Arg45 and Arg53 in mutant 3, and Arg45, Arg53, Lys60, Lys63 and Lys66 in mutant 4). These results were encouraging and implied the ability of the 1cM NLB to bind to multiple locations within the SR-A collagen-like domain, providing a strengthened ability to block oxLDL binding and uptake. In mutant 5 there was no specificity observed and the replacement of all seven residues in the region of interest resulted in the abolishment of specific binding, however the aliphatic chains did again seem to associate with the glycine residues. While there was no *in vitro* site-directed mutagenesis study to reinforce these findings as yet, the ability of the wild-type model to trend with experimental results supports these findings.

The binding energy (Table 2) was computed for each refined 1cM-mutant complex using Equation 1. The most favorable binding was seen with the wild-type SR-A collagen-like domain homology model followed by mutants 4 and 2. Each of these mutants had two residues replaced with alanines and results from this study implied that the mutation of only two residues in the binding pocket did not significantly inhibit binding. The percent change in the binding energy from wild-type SR-A correlated with the number of residues mutated from binding pocket. The correlation between number of residues removed and percent change in the binding energy from wild-type SR-A was linear, with the exception of a sharp spike that correspond to mutant 3 (replacement of Lys60, Lys63 and Lys66 with alanines). This suggested the important role of the lysines in binding between 1cM and SR-A as mutation of these residues had the greatest effect on binding energy. It should be noted that the binding energies of PEG-COOH and 1cM1cP with the mutants followed an identical trend indicating the specific binding of these NLB models, but the 1cP, 0cM, 2cM and 1cM-link had no correlation (data not shown). This is not surprising as only 1cM, 1cM1cP and PEG-COOH appeared to be oriented in a way to facilitate binding in this region (Figure 6 and Figure 8).

Conclusions

NLBs designed to block scavenger receptors and inhibit oxLDL accumulation were examined using both *in vitro* and molecular modeling SAR studies to investigate the interaction between a NLB and SR-A. To the best of our knowledge, this is the first ever modeling SAR study of a nanoparticle or scavenger receptor and has opened the door to numerous future studies. Results indicate that the collagenous domain homology model interactions with NLB models correlated well with *in vitro* studies of THP-1 macrophage and NLB interactions, shown by models with the most favorable (lowest) docked energy having the same chemistry as the NLBs that reduced cholesterol accumulation to the greatest extent. This validated our SR-A collagen-like domain homology model and confirmed the hypothesis that novel NLB designs may be screened for oxLDL inhibitory potential, following prediction. The NLBs containing hydrophobic-bound carboxylate groups (1cM and 1cM1cP) were the most efficient inhibitors of oxLDL accumulation by macrophage cells. It was noted that only the 1cM, 1cM1cP and PEG-COOH models appeared to be oriented in a way so as to facilitate binding in the region consisting of residues Arg45, Arg53, Lys60, Lys63 and Lys66 and were also the only NLB models with favorable energies. These results suggested the importance of organization of anionic charges and hydrophobic moieties in close proximity to the anionic group for efficient receptor blocking as well as implied that the interaction between the receptor and NLB was not solely charge-based.

The creation of mutant models demonstrated the importance of all residues in the collagen-like domain region of interest (residues 45–65) for binding to 1cM. Site-directed mutagenesis experiments will be performed to confirm this hypothesis. Furthermore, the important role of the charged residues as demonstrated by the mutant binding energies may provide opportunities for NLB refinement using information gained from this SAR of NLBs with SR-A. Future studies will focus on the development and use of coarse-grained molecular models to more completely characterize the system of NLB and SR-A interactions.

Acknowledgments

This study was supported grants from the American Heart Association (AHA), National Institutes of Health (NIH) and National Science Foundation (NSF), awarded to Dr. Prabhas V. Moghe. We thank Sarah Sparks, Dr. Jinzhong Wang, and Dr. Kathryn Uhrich of Rutgers Dept. of Chemistry and Chemical Biology for the synthesis of the nanoparticles used in our studies. Nicole Plourde was partially supported by the Rutgers NSF DGE 0333196 IGERT Program on Biointerfaces. We acknowledge access to computational facilities at UMDNJ-Informatics institute and the academic computing services of UMDNJ.

Abbreviations

oxLDL	oxidized low density lipoprotein
NLB	nanolipoblocker
SR-A	class A scavenger receptor
SAR	structure activity relationship
CD36	a class B scavenger receptor
AScM	

	amphiphilic scorpion-like macromolecule
PEG	polyethylene glycol
CMC	critical micelle concentration
0cM	NLB with zero carboxylate on the mucic acid
1cM	NLB with one carboxylate on the mucic acid
1cP	NLB with one carboxylate on the PEG chain
PEG-COOH	NLB with one carboxylate on the PEG chain without aliphatic chains
1cM1cP	NLB with one carboxylate on the mucic acid and one carboxylate on the PEG chain
2cM	NLB with two carboxylates on the mucic acid
MC	multiply-charged
PDB	protein data bank
1Y0FA	structure of collagen type I, chain A

References

- Li AC, Glass CK. Nat Med 2002;8(11):1235–1242. [PubMed: 12411950]
- Berliner J, Leitinger N, Watson A, Huber J, Fogelman A, Navab M. Thromb Haemostasis 1997;78(1):195–199. [PubMed: 9198152]
- Williams KJ, Tabas I. Curr Opin Lipidol 1998;9(5):471–474. [PubMed: 9812202]
- Takahashi Y, Kinoshita T, Sakashita T, Inoue H, Tanabe T, Takahashi K. Adv Exp Med Biol 2002;507:403–407. [PubMed: 12664617]
- Brown MS, Goldstein JL. Annu Rev Biochem 1983;52:223–261. [PubMed: 6311077]
- Steinberg D. J Biol Chem 1997;272:20963–20966. [PubMed: 9261091]
- Kunjathoor VV, Febbraio M, Podrez EA, Moore KJ, Andersson L, Koehn S, Rhee J, Silverstein R, Hoff HF, Freeman MW. J Biol Chem 2002;277:49982–49988. [PubMed: 12376530]
- Yla-Herttuala S, Hiltunen TP. Atherosclerosis 1998;137(Suppl):S81–S88. [PubMed: 9694546]
- Zhang H, Yang Y, Steinbrecher UP. J Biol Chem 1993;268:5535–5542. [PubMed: 8383674]
- de Winther MP, van Dijk KW, Havekes LM, Hofker MH. Arterioscler Thromb Vasc Biol 2000;20(2):290–297. [PubMed: 10669623]
- Platt N, Gordon S. J Clin Invest 2001;108(5):649–654. [PubMed: 11544267]
- Wang X, Greilberger J, Ratschek M, Juergens G. J Pathol 2001;195:244–250. [PubMed: 11592105]
- Yamada H, Kazumi Y, Doi N, Otomo K, Aoki T, Mizuno S, Udagawa T, Tagawa Y, Iwakura Y, Yamada Y. J Med Microbiol 1998;47(10):871–877. [PubMed: 9788810]

14. Boullier A, Friedman P, Harkewicz R, Hartwigsen K, Green SR, Almazan F, Dennis EA, Steinberg D, Witztum JL, Quehenberger OJ. *Lipid Res* 2005;46:969–976.
15. Yoshiizumi K, Nakajima F, Dobashi R, Nishimura N, Ikeda S. *Bioorg Med Chem Lett* 2004;14(11): 2791–2795. [PubMed: 15125934]
16. Guaderrama-Diaz M, Solis CF, Velasco-Loyden G, Laclette JP, Mas-Oliva. *J Mol Cell Biochem* 2005;271(1–2):123–132.
17. Broz P, Benito SM, Saw C, Burger P, Heider H, Pfisterer M, Marsch S, Meier W, Hunziker P. *J Controlled Release* 2005;102(2):475–488.
18. Tian L, Yam L, Zhou N, Tat H, Uhrich KE. *Macromolecules* 2004;37(2):538–543.
19. Harmon AM, Uhrich KE. *J Bioact Compat Polym* 2009;24(2):185–197.
20. Chnari E, Nikitczuk JS, Uhrich KE, Moghe PV. *Biomacromolecules* 2006;7(2):597–603. [PubMed: 16471936]
21. Chnari E, Nikitczuk JS, Wang J, Uhrich KE, Moghe PV. *Biomacromolecules* 2006;7(6):1796–1805. [PubMed: 16768400]
22. Andersson L, Freeman MW. *J Biol Chem* 1998;273:19592–19601. [PubMed: 9677385]
23. Doi T, Higashino K, Kurihara Y, Wada Y, Miyazaki T, Nakamura H, Uesugi S, Imanishi T, Kawabe Y, Itakura H. *J Biol Chem* 1993;268(3):2126–2133. [PubMed: 8380589]
24. Acton S, Resnick D, Freeman M, Ekkel Y, Ashkenas J, Krieger M. *J Biol Chem* 1993;268(5):3530–3537. [PubMed: 8429029]
25. Dejager S, Mietus-Snyder M, Friera A, Pitas RE. *J Clin Invest* 1993;92(2):894–902. [PubMed: 8349824]
26. Chnari E, Tian L, Uhrich K, Moghe PV. *Biomaterials* 2005;26:3749–3758. [PubMed: 15621265]
27. Wang J, Plourde NM, Iverson N, Moghe PV, Uhrich KE. *Int J Nanomed* 2007;2(4):697–705.
28. Chang MY, Potter-Perigo S, Wight TN, Chait A. *J Lipid Res* 2001;42:824–833. [PubMed: 11352990]
29. Oorni K, Pentikainen MO, Annila A, Kovanen PT. *J Biol Chem* 1997;272:21303–21311. [PubMed: 9261142]
30. Wang JM, Cieplak P, Kollman PA. *J Comput Chem* 2000;21(12):1049–1074.
31. Altschul SF, Madden TL, Schaffer AA, Zhang J, Zhang Z, Miller W, Lipman D. *J Nucleic Acids Res* 1997;25(17):3389–3402.
32. Thompson JD, Higgins DG, Gibson T. *J Nucleic Acids Res* 1994;22(22):4673–4680.
33. Orgel JP, Irving TC, Miller A, Wess TJ. *Proc Natl Acad Sci U S A* 2006;103(24):9001–9005. [PubMed: 16751282]
34. Jones DTJ. *Mol Biol* 1999;292(2):195–202.
35. McGuffin LJ, Bryson K, Jones D. *T Bioinformatics* 2000;16(4):404–405.
36. Sali A, Blundell TLJ. *Mol Biol* 1993;234(3):779–815.
37. MacKerell AD, Bashford D, Bellott M, Dunbrack RL, Evanseck JD, Field MJ, Fischer S, Gao J, Guo H, Ha S, Joseph-McCarthy D, Kuchnir L, Kuczera K, Lau FTK, Mattos C, Michnick S, Ngo T, Nguyen DT, Prodhom B, Reiher WE, Roux B, Schlenkrich M, Smith JC, Stote R, Straub J, Watanabe M, Wiorkiewicz-Kuczera J, Yin D, Karplus M. *J Phys Chem B* 1998;102(18):3586–3616.
38. Braun W, Go NJ. *Mol Biol* 1985;186(3):611–626.
39. Case DA, Cheatham TE 3rd, Darden T, Gohlke H, Luo R, Merz KM Jr, Onufriev A, Simmerling C, Wang B, Woods RJ. *Comput Chem* 2005;26(16):1668–1688.
40. Yamamoto K, Nishimura N, Doi T, Imanishi T, Kodama T, Suzuki K, Tanaka T. *FEBS Lett* 1997;414 (2):182–186. [PubMed: 9315682]
41. Jones G, Willet P, Glen RC, Leach AR, Taylor R. *J Mol Biol* 1997;267:727–748. [PubMed: 9126849]
42. Yonath A, Traub WJ. *Mol Biol* 1969;43(3):461–477.
43. Hakansson K, Lim NK, Hoppe HJ, Reid KB. *Structure* 1999;7(3):255–264. [PubMed: 10368295]
44. Otsuka H, Nagasaki Y, Kataoka K. *Curr Opin Colloid Interface Sci* 2001;6(1):3–10.

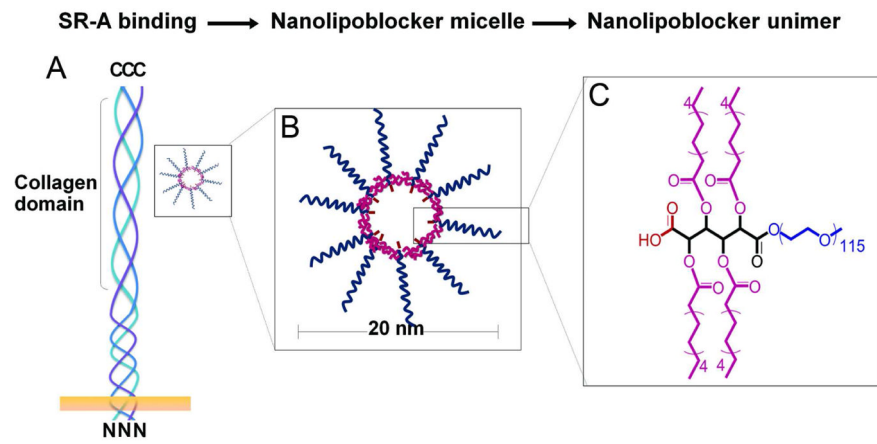
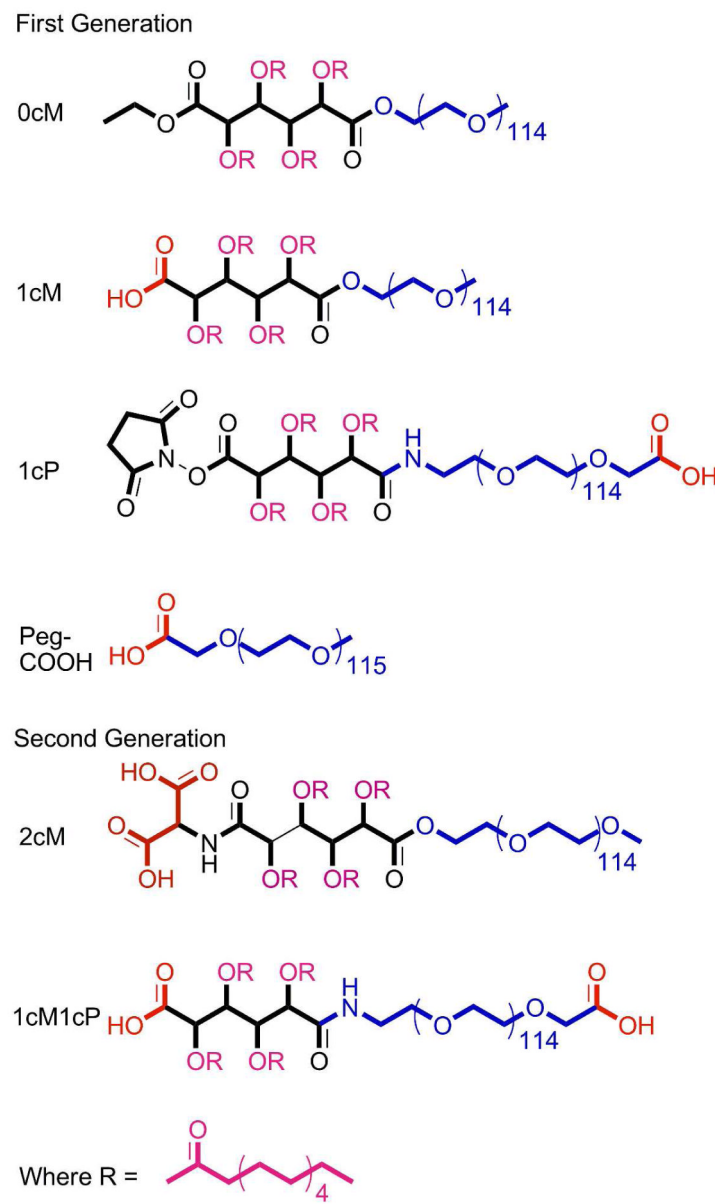
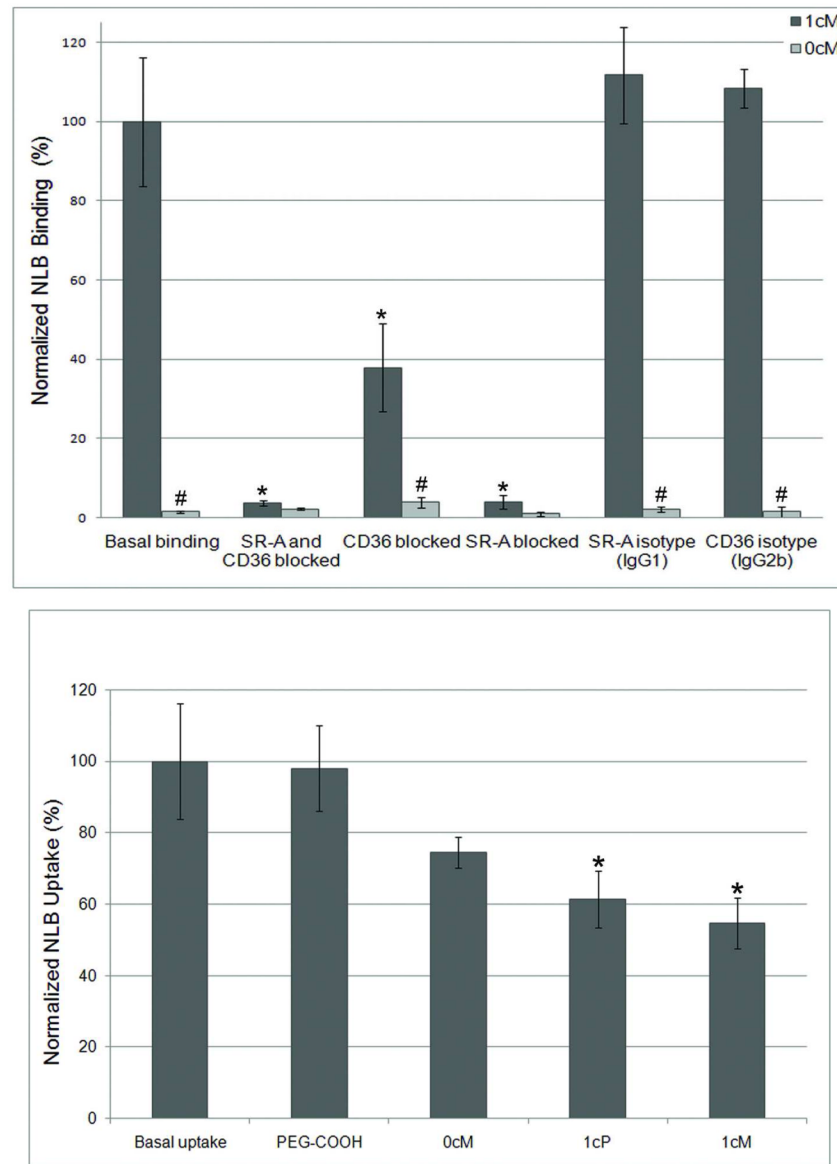


Figure 1.

Nanolipoblockers from (A) the hypothesized binding to the scavenger receptor collagen-like domain, to (B) illustration of nano-sized micellar assembly of (C) nanolipoblocker unimers containing PEG (blue), mucic acid (black), aliphatic acid chains (pink) and anionic carboxylate group (red).

**Figure 2.**

Chemical structure of each of the first generation NLBs and second generation MC-NLBs synthesized and tested. The nomenclature corresponds to the anionic structure: 1cM (1 carboxylate on the mucic acid), 0cM (0 carboxylate on the mucic acid), 1cP (1 carboxylate on the PEG), PEG-COOH (carboxylated PEG), 1cM1cP (1 carboxylate on the mucic acid and 1 carboxylate on the PEG chain), and 2cM (2 carboxylates on the mucic acid).

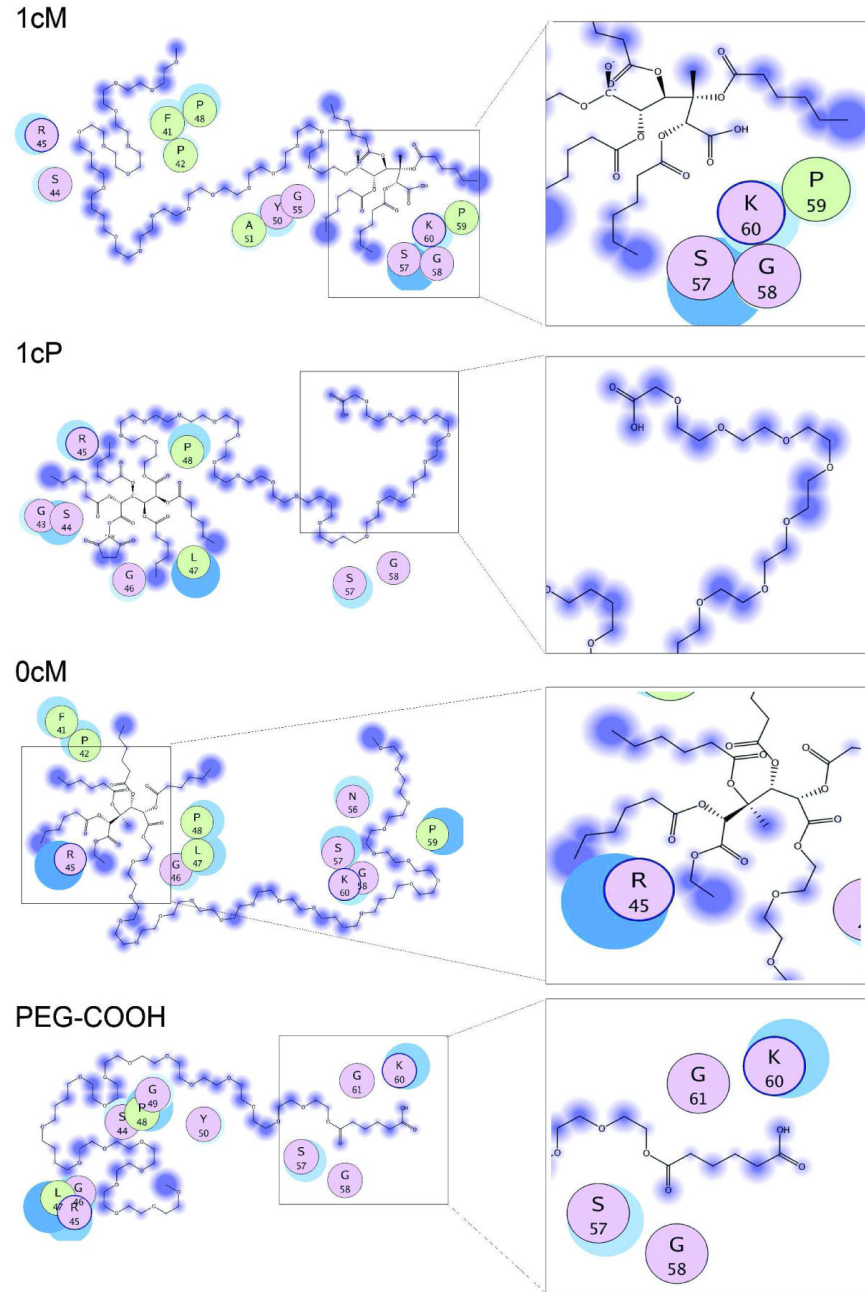
**Figure 3.**

Reduction of NLB binding through receptor blocking illustrates receptor-mediated pathways involved in anionic and neutral NLB uptake by THP-1 macrophages. The symbol * represents significant difference ($P<0.05$) from the basal condition (NLB binding with no receptor blocking). Insignificant variations were confirmed following isotype control antibody blocking. The symbol # represents significant difference ($P<0.05$) between the 1cM and 0cM of a given condition ($n=3$, error bars show the standard error of the mean).

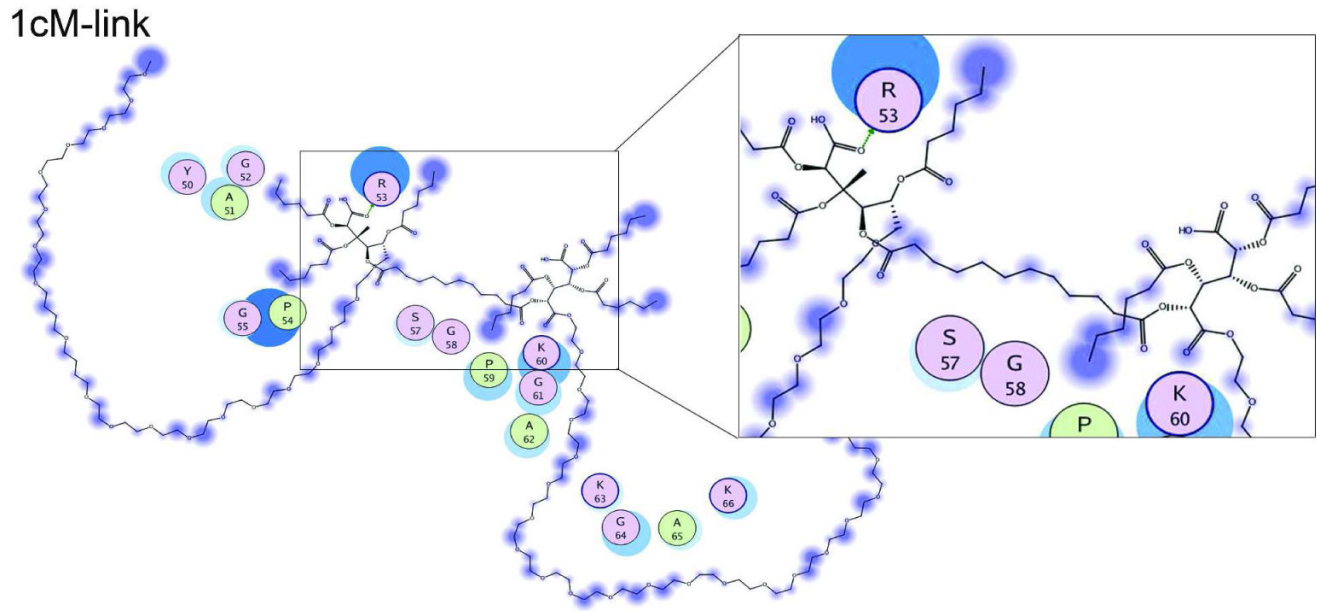
Collagen-like LYOFA	----- AGAXGTPGPQGIAGQRGVVGLXQRGGERGFXGLXGPSGEXGKQGPMSGASGERGPXGPMGP	30 840
	* ***.*.:***: * ** ** ***:***	
Collagen-like LYOFA	PGLKGDRGAIGFPGSRGLPGYAGRPGNSGPKGQKGEKGSG- XGLAGPXGESREGAXGAEGSXGRDGSXGAKGDRGETGPAGPXGAXGAXGAPGPVGPAGK	70 900
	*** * * * *: * * *** . *. ***:***. * ..	

Figure 4.

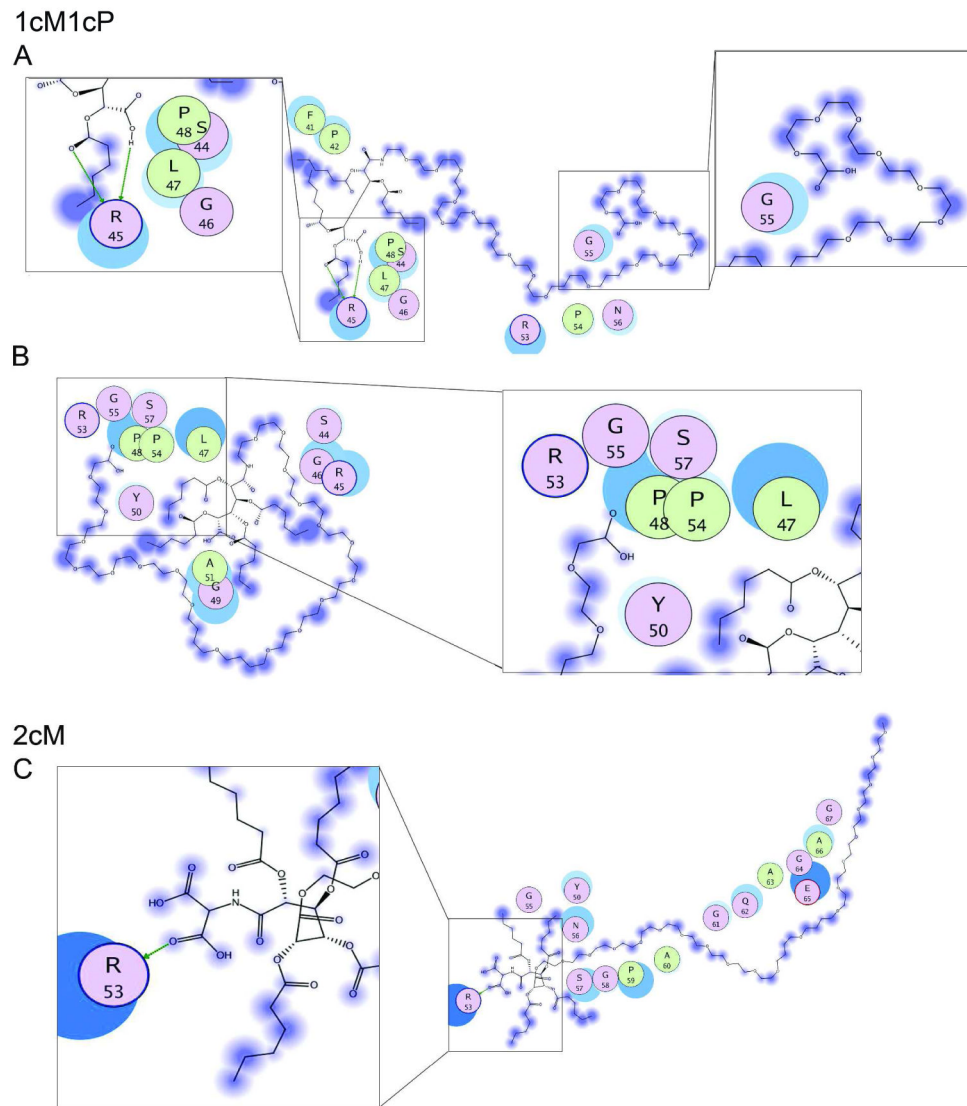
Reduction of oxLDL accumulation in the presence of various NLBs illustrates the structure-activity relationship of NLBs with THP-1 macrophage cells. The symbol * represents significant difference ($P<0.05$) from the basal condition (oxLDL accumulation without NLB) ($n=3$, error bars show the standard error of the mean).

**Figure 5.**

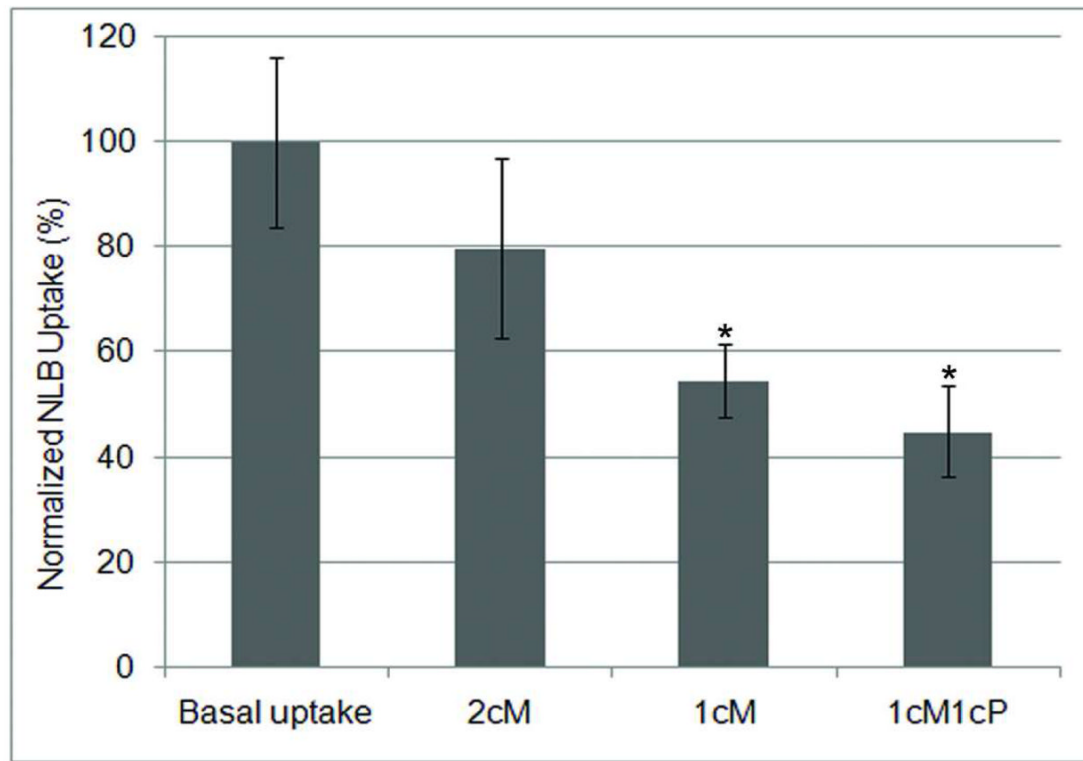
ClustalW pairwise alignment of SR-A collagen-like region and collagen type I chain A (1Y0FA) with the regions necessary for oxLDL binding highlighted in gray boxes.

**Figure 6.**

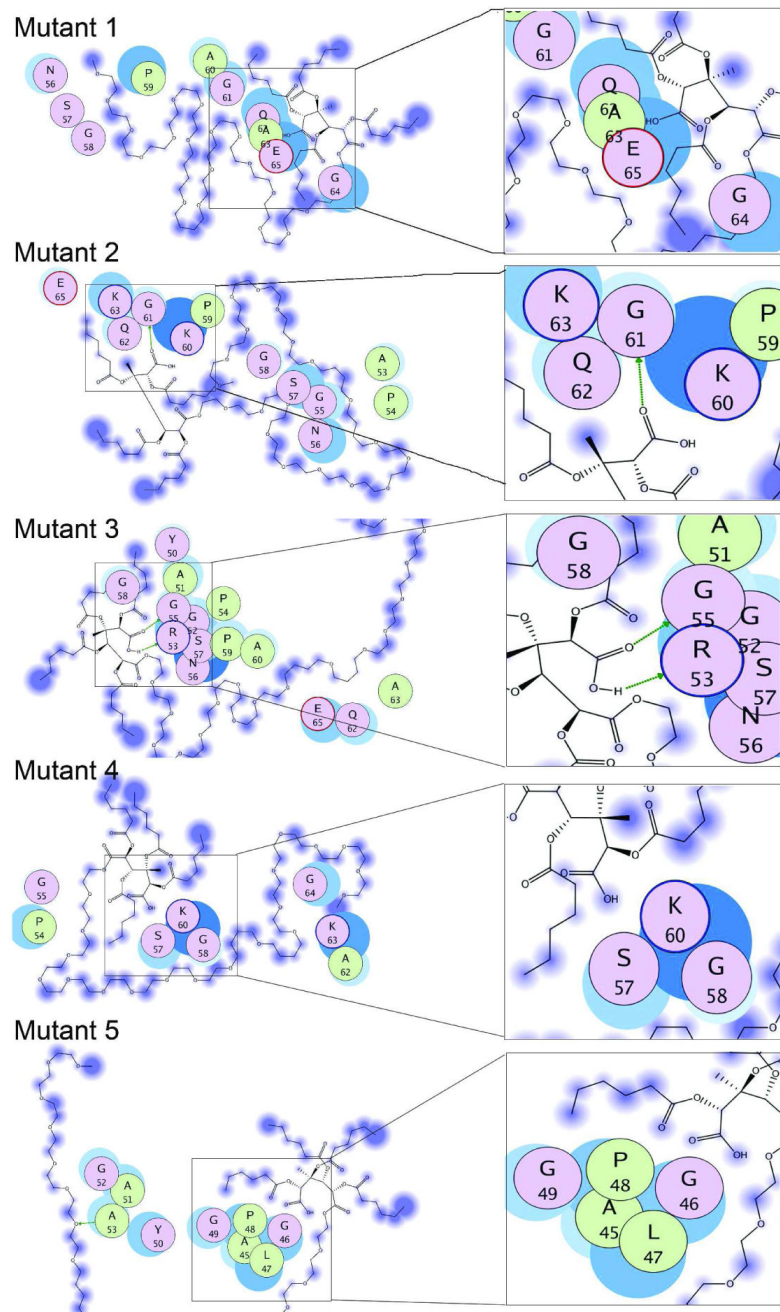
Schematic representation of the docked interactions of SR-A collagen-like domain homology model residues (as seen in the colored circles) with NLB models: 1cM (1 carboxylate on the mucic acid), 1cP (1 carboxylate on the PEG), PEG-COOH (1 carboxylate on PEG), and 0cM (zero carboxylate on the mucic acid). Residue characteristics are illustrated through color: Purple = polar, green = hydrophobic, blue border = basic, and red border = acidic.

**Figure 7.**

Schematic representation of the docked interactions of SR-A collagen-like domain homology model residues (as seen in the colored circles) with NLB model of 2 covalently bonded 1cM unimers representing a section of a 1cM NLB aggregate. Residue characteristics are illustrated through color: Purple = polar, green = hydrophobic, blue border = basic, and red border = acidic.

**Figure 8.**

Schematic representation of the docked interactions of SR-A collagen-like domain homology model residues (as seen in the colored circles) with MC-NLB models: 1cM1cP (1 carboxylate on the mucic acid and 1 carboxylate on the PEG). A. In 70% of docking runs, the 1cM1cP model was found to bind as mode A to distant residues, B. in 30% of runs as seen in mode B, the MC-NLB folded inward and bound the same or adjacent residues. C. Schematic representation of the interaction of 2cM (two carboxylates on the mucic acid) with SR-A. Residue characteristics are illustrated through color: Purple = polar, green = hydrophobic, blue border = basic, and red border = acidic.

**Figure 9.**

The reduction of oxLDL accumulation in the presence of MC-NLBs compared to the previously identified most inhibitory NLB configuration (1cM). The symbol * represents significant difference ($P<0.05$) from the basal condition (oxLDL accumulation without NLB) ($n=3$, error bars show the standard error of the mean).

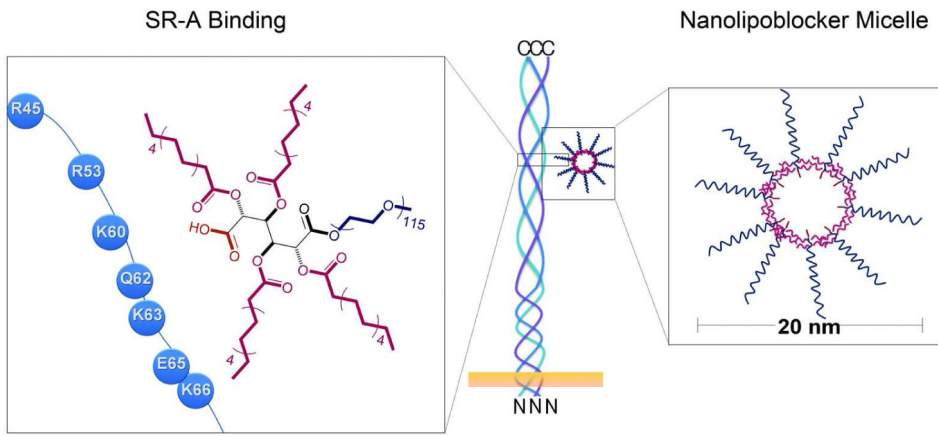


Figure 10.

Schematic representation of docked interactions of 1cM NLB model with SR-A collagen-like domain homology model mutants in which specific residues were replaced with alanine: mutant 1(Arg45, Arg53, Lys60, Lys63, and Lys63), mutant 2 (Arg45 and Arg53), mutant 3 (Lys60, Lys63, and Lys63), mutant 4 (Gln62 and Glu65), mutant 5 (Arg45, Arg53, Lys60, Lys63, Lys63, Gln62 and Glu65). Residue characteristics are illustrated through color: Purple = polar, green = hydrophobic, blue border = basic, and red border = acidic.

Table 1

Values of the binding energy of first and second generations of NLB models when docked with SR-A collagen-like domain homology model

First Generation NLB	ΔE binding (kcal/mol)
1cM	-42.07
PEG-COOH	-23.83
1cP	20.45
0cM	38.88
1cM-link	283.46
Second Generation MC-NLB	ΔE binding (kcal/mol)
2cM	40.92
1cM1cP	-59.99

Table 2

Values of the binding energy of the 1cM model when docked with SR-A collagen-like domain homology model mutants as well as the percent change in binding energy from wild-type SR-A collagen-like domain homology model versus the number of residues mutated. mutant 1(Arg45, Arg53, Lys60, Lys63, and Lys63), mutant 2 (Arg45 and Arg53), mutant 3 (Lys60, Lys63, and Lys63), mutant 4 (Gln62 and Glu65), mutant 5 (Arg45, Arg53, Lys60, Lys63, Lys63, Gln62 and Glu65)

SR-A Mutation1cM	ΔE binding (kcal/mol)	Percent change from Wild-type SRA	Number of residues mutated to Alanine
Wild type	-42.07	0	0
Mutant 1	1.15	102.73	5
Mutant 2	-31.09	26.10	2
Mutant 3	65.61	255.95	3
Mutant 4	-32.19	23.48	2
Mutant 5	30.87	173.38	7